



## Prototyping Roof Mounts for Photovoltaic (PV) Panels: Design, Construction and CFD Validation

Mohammad AL-Rawi<sup>1,\*</sup>, Nived Rajan<sup>2</sup>, Sreeshob Sindhu Anand<sup>3</sup>, Tony Pauly<sup>4</sup>, Nikhil Thomas<sup>5</sup>

<sup>1</sup> Centre for Engineering and Industrial Design, Waikato Institute of Technology, Hamilton 3240, New Zealand

<sup>2</sup> Motus Hydraulics Ltd, Hastings 4120, New Zealand

<sup>3</sup> Service Engineering Group (SEG) Ltd, Tauranga 3112, New Zealand

<sup>4</sup> Designer Homeware (NZ) Ltd, Tauriko 3171, New Zealand

<sup>5</sup> Domett Truck and Trailer, Tauranga 3110, New Zealand

### ARTICLE INFO

#### Article history:

Received 28 December 2021

Received in revised form 6 February 2022

Accepted 7 February 2022

Available online 24 February 2022

#### Keywords:

Building-integrated Photovoltaic (BIPV) Panels; CFD; Roof Mounting

### ABSTRACT

Many countries have committed to using renewable energy and increasingly encourage the use of solar panels in residential dwellings part of achieving sustainability goals. However, building regulations and standards are often slow to catch up. In New Zealand, there is no specified standard for the mechanical structure when mounting the solar panels to the roof. Solar panel mounts can cause significant damage to the roof in the presence of environmental stressors, such as heavy rain and high-speed wind gusts. This paper presents the process of designing a novel mounting unit for solar panels using computational fluid dynamic (CFD) tools to prototype the unit. The prototype unit is easy to install and can accommodate a range of solar tiles manufactured by leading manufacturers. The proposed mount design addresses issues identified with current mounts, such as roof leaks, tilting of the tiles, and corrosion of mounting units by design optimization and proper material selection. Additionally, we compare the maximum temperature for each part of the unit to the CFD results and come up with an average error of 3.14-3.82%.

## 1. Introduction

Recently many countries have committed to expanding the uptake of renewable energies, and divestment of non-renewable energy-generating assets [1-4]. Part of this process involves encouraging those in private residential dwellings to install Photovoltaic (PV) panels, commonly referred to as solar panels, on their houses to move toward “green” energy production and consumption. Solar-generated power at the household-level has the additional advantage of reduced ongoing energy costs (although it involves a higher up-front cost). Therefore, demand for PV panels is increasing as societies endeavor to become more sustainable [5]. The rooftop of a building is the most common choice for mounting the panel, due to the roof’s exposure to sunlight, and its robust structure which can support the panel’s weight [6]; it also represents the most abundant “unused” real-estate for most households in urban and suburban settings.

\* Corresponding author.

E-mail address: [mohammad.al-rawi@wintec.ac.nz](mailto:mohammad.al-rawi@wintec.ac.nz) (Mohammad AL-Rawi)

<https://doi.org/10.37934/cfdl.14.2.5971>

Many different factors must be taken into account when installing PV panels, including safety, cost-effectiveness, optimal sun exposure and whether the PV panels can accommodate the expected wind load and adverse weather [7]. It is expected that these adverse conditions will increase in severity in future, due to global climate change [7]. Although these parameters have been addressed in the last 10 years, in New Zealand there is no current standard or government regulation on installing either the mounting or the panel itself on the roof [7]. In residential buildings, PV panels are typically installed on the roof [6] which, while it is available space, is the most wind and weather vulnerable structure of the dwelling [7]. Severe weather conditions, such as heavy rain and wind generate lift in the PV panels, hence suction pressure on the roof surface which could damage the cladding and the main structure of the roof [7].

One of the major challenges in installing panels on the roof in the southern hemispheric region is severe weather which has a significant impact on the lifespan of buildings. One of the major issues with PV panel installations is the uplift of roofing structures that they create. Meroney and Neff [6] used Computational Fluid Dynamics (CFD) methods to calculate the wind load on the structure considering the drag and lift forces created by the panels and identified the maximum load which the structure can endure without causing damage. Cao and Yoshida [8] presented a detailed study of wind load resistance and wind pressure measurement for a flat-roofed building under a single array setup and multi-array setup. They found the effect of distance between arrays and the effect of building depth were very important when designing the PV panel installation. Additionally, the negative module force coefficients for single-array cases were much larger than those for multi-array cases due to the tilt angle and distance between arrays which increase the negative module forces [8]. Bellavia [9] developed a light-weight PV roof tile for sloping roofs which also demonstrated hurricane resistance, featured a specialized coating for fire resistance, were flexible/moldable, had the ability to withstand the external load, as well as ease in installation [9]. Aly *et al.*, [10] conducted a substantial study (experimental and computational) on using PV panels to reduce the uplift caused by wind on gable-roofed low-rise buildings provides specific valuable insights adopted in the panel's technology. It lists the advantage of having a backup solar power source after an immediate power outage, especially after a thunderstorm.

Another factor that plays an important role in solar panels installation and usage is the cost. Many studies [11-13] focus on examining the influence of risk and uncertainty on overall costs associated with the system. Wittbrodt and Pearce [13] identified that an 80% reduction in cost and 33% increase in power density could be achieved via their novel low-weight PV racking system for commercial rooftops based on crossed cables. Their comparison took into account capital costs, labor cost and installation including technical specifications. Peng *et al.*, [14] highlight the importance of upgradability of PV panels, given the speedy evolution of the technology which means the panel will need to be upgraded multiple times during the lifespan of the building. Therefore, not only cost but also ease of access to the mounts should be considered, as well as minimal damage to the building/roof structure is required when changing the panel.

Furthermore, the PV panel can be obscured by particulate accumulation. Lu and Zhang [15] studied computationally the effects of different Reynolds numbers and roof inclinations on deposits of dust on the PV system when mounted on building roof. They found the main solution was manual or mechanical cleaning of the PV array using water. This is particularly important for low rainfall areas.

Installation of the PV panel can damage the roof-structure through corrosion of the mount. This is caused by weathering of the metal components in the panel's mounting unit, which may eventually lead to considerable structural damage of the roof. Whitmore [16] presented an innovative technology that uses an Anode sacrificially for the protection of Cathode from corrosion. An activator

further enhances the corrosive nature of the Anode material to ensure continuous protection of the Cathode material from corroding. This activator could be included in the material used for ionic conduction by fillers such as gels or liquids with alkali hydroxides. Causes of corrosion, such as humidity, or the presence of certain elements in the atmosphere like Sulphur Dioxide (SO<sub>2</sub>), or the salts of Chloride were investigated in ref. [17]. The research indicates that 'aerosols' in Chloride play a significant role in corrosion [17, 18]. Construction materials can also impact on corrosion. For example, Nürnberger and Köse [18] found that Timber, being a porous material, is an excellent host for moisture as well as acidic corrosive agents from the atmosphere, all of which increase the pace corrosion. They further investigate the self-metallic and bi-metallic corrosive behavior of Aluminum and Stainless Steel, finding that these are superior to Timber as mounting structures, due to Timber's water-retaining feature.

Fedorova *et al.*, [19] presented a methodology for testing the degree of wind-driven rain ingress in building-integrated photovoltaic (BIPV) systems, in a laboratory setting (wind speed ranges from 12.9-35.3 m/s). They focused on collecting data on the amount of leaked water collected during the experiment using climate conditions prevalent in Europe. Wind-driven rain exposure was applied up to extreme levels, including hurricane wind speeds of up to 35.3 m/s. Their study focuses on quantifying water intrusion during the severe conditions, and they noted that this was significantly affected by the amount of rubber sealing applied, and the potential for deformation of the seals during installation. Also, Pearce *et al.*, [20] presented a modification based on an open-source design in which conventional PV modules were converted to BIPV roofing slates via direct mounting, which achieved a 20% total cost reduction.

Baumann *et al.*, [21] compared the energy yield of vertically mounted bifacial (east-west facing) modules combined with a green roof to the reference model of a south-oriented monofacial module. The vertically mounted modules were found to obtain comparable specific energy yields (kWh/kWp) to those of monofacial flat roof installations. Kurnik *et al.*, [22] provide a theoretical analysis and experimental testing of different mounting and operating conditions for the PV modules. They assessed the impact of open rack, ventilated or unventilated roof mounting, amongst others, as well as the effect of wind speed under different module type. Their simulations revealed negligible impact of the irradiance, wind speed and mounting conditions of the module: the module's relative temperature difference being approximately equal to the conversion efficiency, under the different formations.

The fundamental issues reviewed are damage to the structure due to wind and the resulting uplift, snowfall obscuring the PV units, corrosion of the metallic components, and leakage. Previous studies [23, 24] shed light on specific solutions for the identified issues. Additionally, certain cutting-edge technologies such as the novel kesterite technology [25, 26] and conversion of commercial ceramic tiles for BIPV [20, 24] purposes are also identified, which require further research. In the past, the design of the PV panels themselves have received significant attention [27]; however, the design and analysis of panels' mounting unit [28] have not received much attention. Therefore, the main aim of our study is to design and prototype a roof mounting unit that addresses the roof leakage issues, including those related to the mount itself (such as corrosion and damage to the roof), and those relating to the behavior of the PV panels (such as tilting and uplift) due to weather conditions.

## 2. Methodology

Currently, the waterproof tile support panels can be screwed into purlins, and this acts as a waterproofing membrane and gives an insulated finish. The challenge here is to investigate an ideal waterproofing membrane with the following material properties: (i) high tensile strength to resist

tearing; (ii) lightweight so easily applied; (iii) whether protection and rainproof and (iv) high fire resistance. In this section, we will present the concept of the design using flow simulation tools to perform CFD and FEA analysis and present the final prototype of the mounting unit.

Using a simulation-driven design allowed us to reduce product development cost and time. The methodological approach consists of combined CFD and FEA analysis to arrive at the most promising design that eliminates issues explored in the introduction section. This process is outlined in Figure 1.

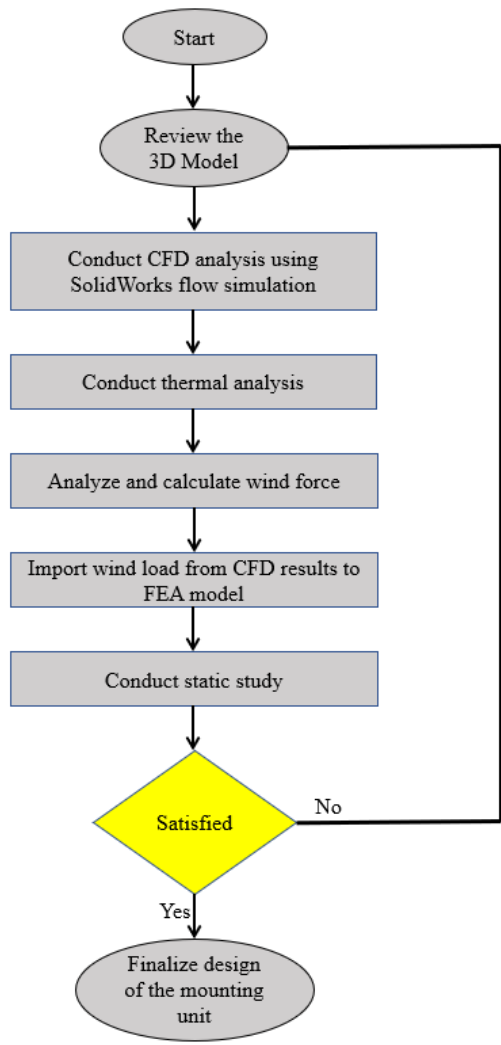
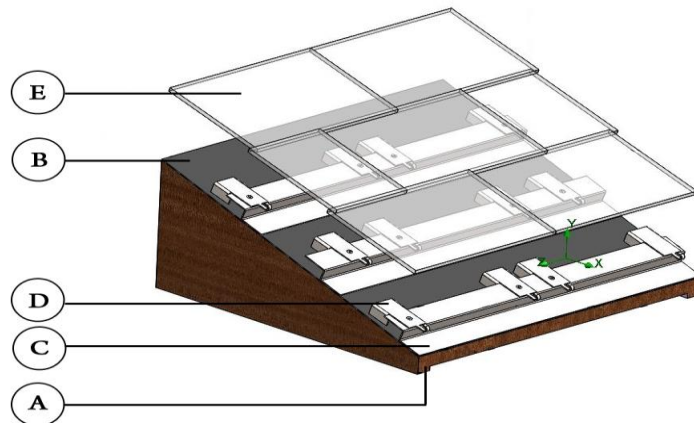


Fig. 1. Flow chart for the design model validation

### 2.1 Design of the Unit

The roof-mounted PV panels could vary considerably in terms of their overall dimension; however, the majority of the PV panels available in the market are square shaped (200 x 200 x 10 mm), so our preliminary design is based on the following two assumptions: (i) that 30 mm clearance is sufficient to accommodate all the electrical wirings; (ii) material properties are based on the American Society for Testing and Materials (ASTM) international standard. Therefore, we came with the following ideal clamping unit that minimises the risk of roof fire (related to the electrical circuitry), leakage around the mount, tilting of the mounting unit and corrosion issues associated with PV panels as shown in Figure 2. In this figure, the timber roof was chosen based on three most popular

shapes in New Zealand are the hip roofline, the gable roofline, the flat roof, and the mono-pitch. The design presented below resembles a mono-pitched roof with an angle of  $68^\circ$ . As the name implies, a mono-pitched roof has just one slope. Mono-pitched roofs are very cost-effective and are widely seen in New Zealand. We have used a waterproofing membrane consisting of a waterproofing sheet laid above the rooftop that does not allow water to seep through and eliminates the roof leakage issues due to the installation of battens. The selected material for the water-proofing membrane is Butynol. Butynol is a synthetic rubber membrane which is resistant to degradation from heat and sunlight/solar radiation. It has a high gas impermeability, is tough but remains flexible at high and low temperatures, is water-impermeable and defends against acids, and chemicals; hence it is an ideal choice to counteract rooftop leakage. The chemical structure depiction of Butynol is  $C_4H_9OH$ . The thickness of the waterproofing membrane is 1.5 mm, and it has a potable water feature based on the standard AS/NZS 4020:2018. The overall dimensions of the waterproofing membrane is 600 x 600 x 1.5 mm. The solar tiles overall dimension is 300 x 200 x 8 mm. Integrated PV tiles are not readily available in the New Zealand market, so the thin solar film is added to the top of the ceramic tile to create photovoltaic tiles, or PV tiles.



**Fig. 2.** The proposed design: (a) wooden roof; (b) water proofing membrane; (c) battens; (d) link channels and (e) solar tiles

The link channels shown in Figure 1 (d) are designed with a secured locking mechanism which spaces the batten so as to accommodate the PV tiles, as shown in Figure 3. Each link channel is also essential to protect the roof: in the event of high rainfall, excess rainwater flows into the link channel then out onto the tile below. This also keeps the area relatively free from debris. The link channel material is Stainless Steel grade SS316.

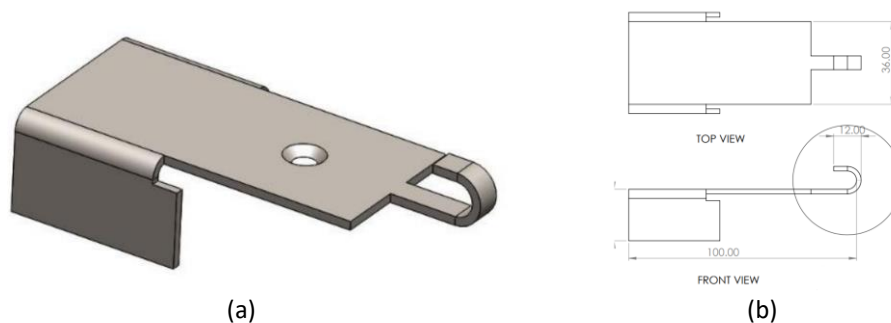


**Fig. 3.** Link channel (a) isometric view and (b) the top and front view with dimensions

The battens function to secure the link channels and PV tiles onto the roof. The innovative design of the batten allows for a roof pitch as low as  $5^\circ$ . This assists with weather-tightness of the area and keeping it clear from debris, as shown in Figure 4. In this design, the battens are 600 mm in length, and the material is chosen to be Stainless Steel grade 316. The screws which secure the link channels with the battens are M3 x 10 mm Stainless Steel grade 316.

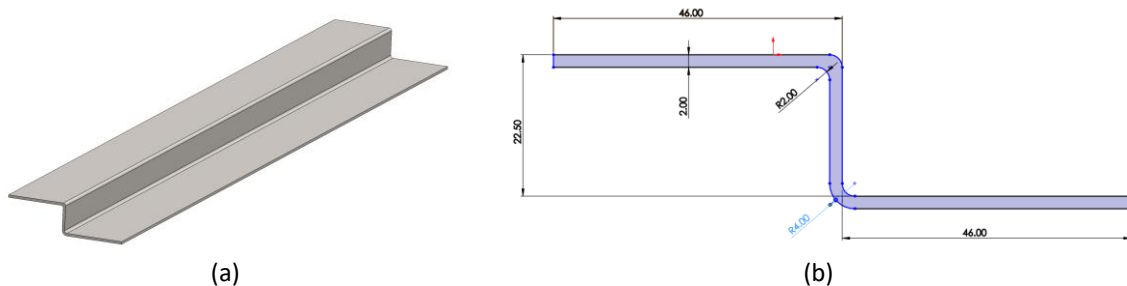


**Fig. 4.** The batten (a) isometric view (length 600 mm) and (b) front view with dimensions

To perform a comparison with the design presented in ref. [20] the batten we present has a shorter length, of 600 mm as shown in Figure 4 (a), and is constructed with curved edges of radius 2 mm as shown in Figure 4 (b), to reduce vortices in air-flow past the structure. The link channel, as shown in Figure 3 (a), is then screwed on top of the batten, allowing a space to let the water slide over the Butynol mat so that the water remains uncontaminated. Based on ref. [20], it is recommended to add an aluminum channel, as flashing to prevent water ingress at the head of the BIPV roofing system. The advantages of our design is that the batten is not undermined by high wind speeds, uses natural ventilation to prevent moisture build-up, and maintains potability of rainwater so can be used in conjunction with rainwater collection systems.

## 2.2 Minimisation of Overheating

As shown in Figure 5, a small fraction of the PV tiles' surface is in contact with the link channels and battens. When a heat flux is imposed by the tiles, the uniform flow of heat is generally restricted to conduction through the contact spot. The limited number and size of the contact spot results in an actual contact area that is significantly smaller than the apparent contact area. The limited contact area between the link channel and battens causes a thermal resistance.

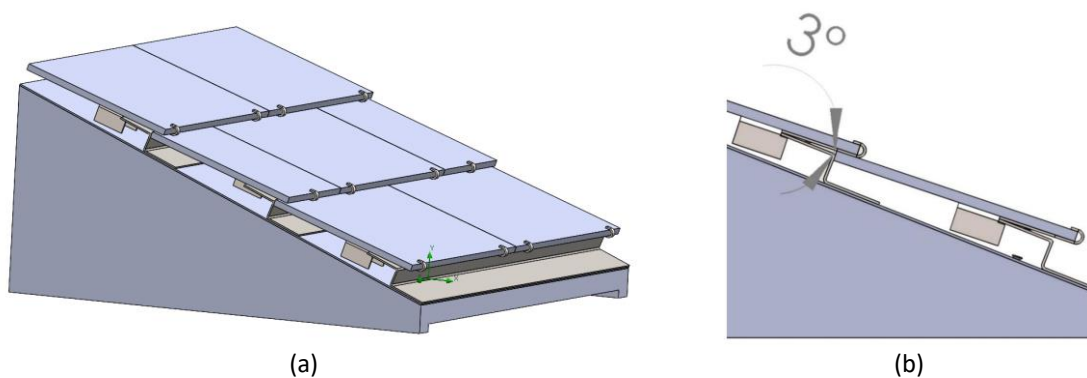


**Fig. 5.** (a) the isometric view for the CAD model and (b) the two materials in contact with a  $3^\circ$  angle

The temperature difference used to define the contact resistance at the junction is based on the thermal joint model implemented in Flow Simulation. This equation determines risk of overheating

on the roof by identifying, in the CFD model, the heat transfer from one “hot” surface to the other “cold” surface, using Eq. (1)

$$Q = \alpha(T_1 - T_2) \tag{1}$$

where  $T_1$  is the temperature of the link channel,  $T_2$  is the temperature of the battens, and  $\alpha$  is the heat transfer coefficient. Additionally, Eq. (1) could be used for the PV tiles and the other parts of the mounting units. The PV tiles, which are solar panels designed to look like and function as a conventional roofing tile, have the material properties as shown in Table 1.

The Flow Simulation determines the heat transfer in solid and fluid media, taking into account the energy exchange between them. Using the energy conservation theory, the heat flux (wall to ambient and wall to environment wall) can be determined using Eq. (2).

$$Q = \alpha(T^4 - T_{out}^4) \tag{2}$$

where  $T_{out}$  is the temperature of the environmental radiation. The energy exchange between the fluid and solid media is calculated via the heat flux in the direction according to the solid/fluid interface taking into account the solid surface temperature and the fluid boundary layer characteristics.

**Table 1**  
 Material properties for the tile

| Property             | Value    | Units             |
|----------------------|----------|-------------------|
| Elastic Modulus      | 6.8935e4 | N/mm <sup>2</sup> |
| Poisson’s Ratio      | 0.23     | -                 |
| Mass Density         | 2457.6   | kg/m <sup>3</sup> |
| Tensile Strength     | 12       | N/mm <sup>2</sup> |
| Yield Strength       | 1.723e2  | N/mm <sup>2</sup> |
| Thermal conductivity | 0.749    | -                 |

### 2.3 Elimination of Corrosion

Stainless steel grade 316 has almost the same physical and mechanical properties as grade 304; however, grade 316 comprises an additional element known as molybdenum, which has greater corrosion resistance, particularly against chloride and components of acid rain as shown in Table 2 and the material properties as shown in Table 3.

**Table 2**  
 Material composition of grade 316

| Composition     | SS316 (weight %) |
|-----------------|------------------|
| Carbon (C)      | 0.08 Max         |
| Manganese (Mn)  | 2.00 Max         |
| Phosphorus (P)  | 0.045 Max        |
| Sulphur (S)     | 0.03 Max         |
| Silicon (Si)    | 0.75 Max         |
| Chromium (Cr)   | 16.00-18.00      |
| Nickel (Ni)     | 10.00-14.00      |
| Molybdenum (Mo) | 2.00-3.00        |
| Nitrogen (N)    | 0.1 Max          |
| Iron (Fe)       | Balance          |

**Table 3**  
 Material properties for Stainless Steel -SS316

| Property         | Value   | Units              |
|------------------|---------|--------------------|
| Elastic Modulus  | 1.929e5 | N/mm <sup>-2</sup> |
| Poisson's Ratio  | 0.27    | -                  |
| Mass Density     | 8000    | kg/m <sup>-3</sup> |
| Tensile Strength | 580     | N/mm <sup>-2</sup> |
| Yield Strength   | 1.723e2 | N/mm <sup>-2</sup> |

### 3. Thermal Analysis

We perform thermal analysis using Flow simulation to investigate the temperature distribution and temperature gradient, as well as the amount of heat exchange between the mounting unit and its surrounding environment. The thermal analysis was set to solve conduction and convection equations embedded in Flow simulation. The air temperature was set to 10°C, the wind velocity to 13 m/s and pressure to 101.325 kPa. The conduction was accountable for the heat flow inside the PV tile (having material properties as shown in Table 1) unit and for the convection was accountable for heat entering and escaping through a medium (air). Figure 6 shows the control volume boundary conditions with respect to the heat conducted through the wall from the higher to the lower temperature. As evident in Figure 6, heat dissipated by convection always requires the movement of the fluid surrounding the body.

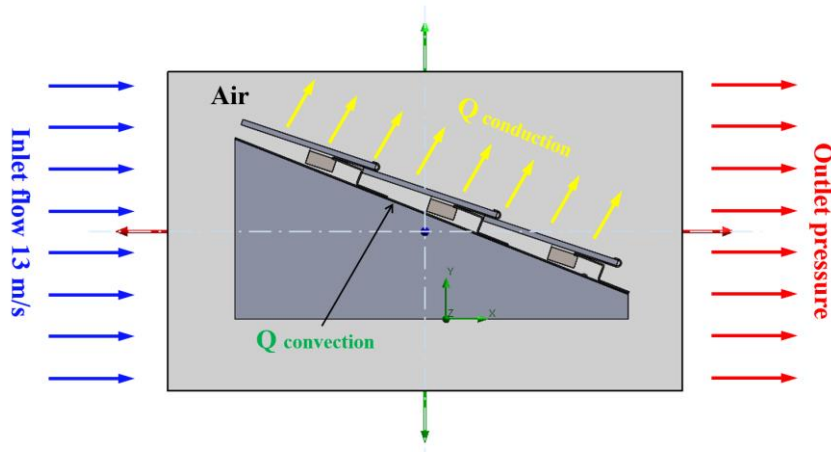


**Fig. 6.** Control volume boundary conditions

### 4. Convergence Study

The mesh quality plays a significant role in the result type, so a mesh convergence study was performed. The mesh convergence study was conducted with different sizes of the mesh (course, medium and fine). The effects of each mesh on the displacement result was compared to achieve the convergence of the study. Figure 7 shows the displacement reading with respect to the degrees of freedom. An 0.233% error was within the acceptable range to the displacement.



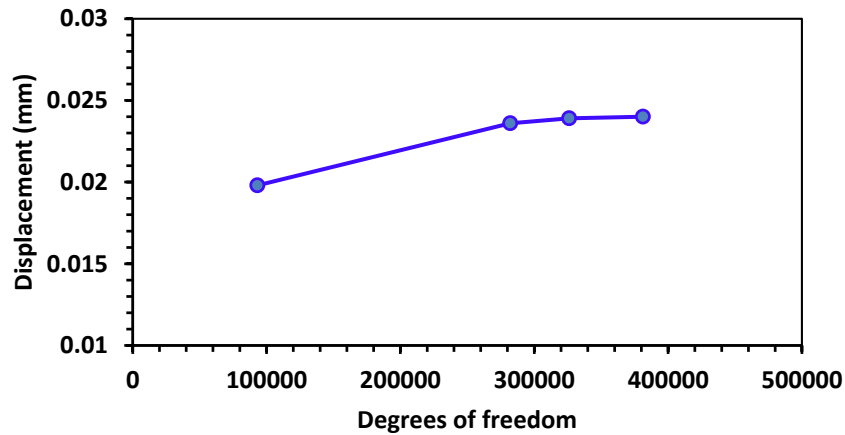


Fig. 7. Conditions Displacement vs degree of freedom

### 5. Results and Discussion

Heat conduction of the solids was selected because PV tiles generate heat, and we are interested to know how the heat is dissipated through the battens and link channels and then out to the fluid.

The system is exposed to the surrounding environment, with an average air temperature of 10°C, and the air circulation significantly contributed to the cooling. The limited contact area between the battens and the link channel creates a thermal contact resistance. By looking at the cut plot of the thermal analysis, we can see that when the tiles’ temperature is at 50°C the roof temperature remains 10.68°C. Figure 8 depicts the maximum and minimum temperatures of each component in the assembly based on the heat emanating from PV tiles. Table 4 shows the maximum and minimum temperatures for each component in the unit.

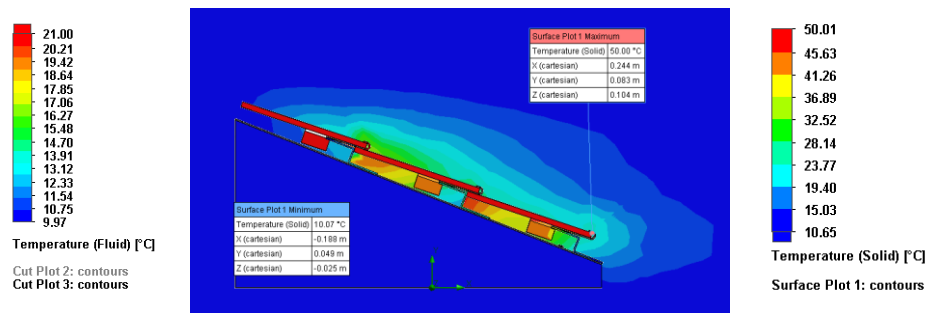


Fig. 8. Temperature contours for the unit

Table 4

Temperature of each component in the unit

| Name of Component   | Maximum Temperature (°C) | Minimum Temperature (°C) |
|---------------------|--------------------------|--------------------------|
| Solar tiles         | 50                       | 47.62                    |
| Link channels       | 26.91                    | 26.87                    |
| Battens             | 16.78                    | 15.92                    |
| Waterproof membrane | 13.21                    | 12.5                     |
| Roof                | 11.20                    | 10.67                    |

In the study, the pressure distribution contours were investigated, as shown in Figure 9. This figure shows the pressure distribution on all faces of the solar tiles in contact with the fluid medium

(air). As shown in Figure 9, the maximum pressure is 102.429 kPa and the minimum pressure 100.661 kPa.

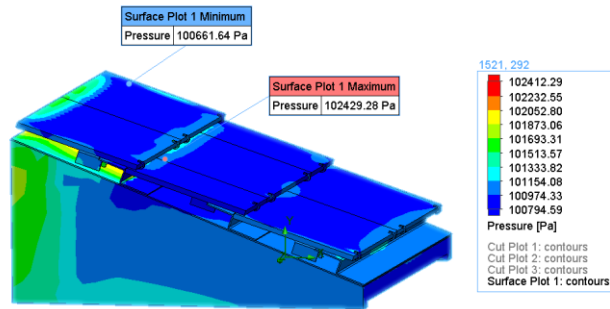


Fig. 9. Pressure contours for the unit

We also investigated the displacement contours for the FE model. Figure 10 (a) illustrates the displacement contours and reaction force of the static study within the isometric view, while Figure 10 (b) shows the side view with a maximum obtained displacement of 0.024 mm.

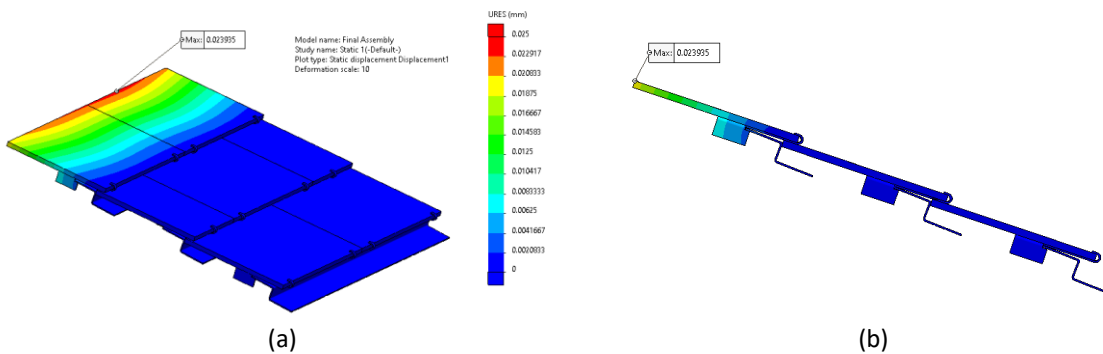


Fig. 10. Displacement contours for the unit: (a) isometric view and (b) side view

The Von Mises stress contours were also investigated, to determine whether the material will yield or fracture. The results are shown in Figure 11, where the maximum obtained Von Mises stress plot value is 5.652 MPa, which is much lower than the yield strength of the assigned materials.

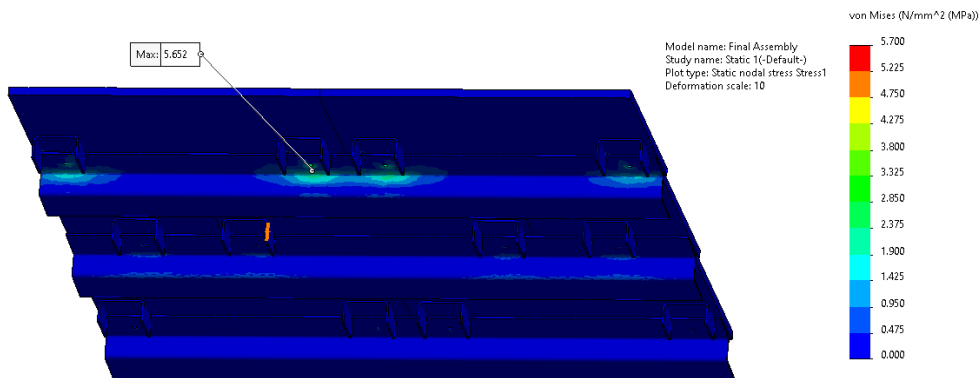


Fig. 11. Von Mises stress contour

Virtual testing using CAD software helped us analyze the design, measure the performance, and make decisions to improve the design before the fabrication stage. Thermal analysis using flow simulation enabled us to identify the heat transfer within the solid bodies. The thermal analysis plot proved that the convection coefficient is heavily dependent on the fluid in the surrounding area. Thermal analysis using Flow simulation also demonstrated the thermal contact resistance between the link channels and battens, which restricts the heat transfer between the solid bodies.

The static design study, using the imported data from the CFD analysis, proved that the design could withstand a wind load of 13 m/s.

To understand how the heat is dissipated from the PV tiles, an external source heats the tile to 50°C for up to 10 minutes, as shown in Figure 12. An infrared temperature measuring device is used to measure how the heat is dissipated from the solar tiles. The surface temperatures of battens, link channels, and the wooden roof were recorded and compared to the CFD results, with an average error of 3.46%, as shown in Table 5. The limited contact area created contact resistance, and the gap between the link channel and roof allowed valuable airflow, hence heat is not transferred to the roof. Also, a water leak test revealed that the clamping unit does not allow water to seep through the tiles. When the water hits the tiles, the excess water flows into the link channel then out onto the tile as shown in Figure 12, keeping the roof and waterproofing membrane dry and free from debris. In addition, we evaluated the total approximate cost at U.S.\$23.67/module in 2021 which does not differ much from the BIPV roof-mounted system which costs U.S.\$22/module as of 2017[20].



**Fig. 12.** Water leakage test

**Table 5**

Temperature in different components compared to the CFD

| Name of Component   | Maximum Temperature (°C)<br>Prototype | Maximum Temperature (°C)<br>CFD model | Error % |
|---------------------|---------------------------------------|---------------------------------------|---------|
| Solar tiles         | 48.3                                  | 49.87                                 | 3.14    |
| Link channels       | 25.88                                 | 26.91                                 | 3.82    |
| Battens             | 16.19                                 | 16.78                                 | 3.51    |
| Waterproof membrane | 12.8                                  | 13.21                                 | 3.1     |
| Roof                | 10.78                                 | 11.2                                  | 3.75    |

## 6. Conclusions

Heat can reduce the output efficiency of the PV tiles installed on a roof by 20-25%. As the temperature of the PV tile increases, its output current rises exponentially, while the output voltage

is reduced linearly. Our mount design allowed a 30 mm air vent, which improved air circulation and cooled down the PV tiles, increasing the output efficiency.

The design also demonstrated that generated heat is not transferred into the roof. The limited contact area between the link channel and batten causes thermal resistance; this reduces the heat transfer to the roof and minimises the risk of roof fire.

The innovative design of our roof mounts avoids tilting of the PV tiles due to heavy wind. The mounting unit is designed to take a wind load of up to 13 m/s. The link channel acts to securely lock the tiles

The Stainless Steel grade SS316 material, used to fabricate the mounting unit, contains a combination of iron, chromium, manganese, silicon, carbon, and significant amounts of nickel and molybdenum, which prevents corrosion issues. The 300 series stainless steels are resistant to scaling and retain strength at high temperatures. The only drawback of stainless steel is its high initial cost.

Future work will include a comprehensive computational and experimental study to assess the condensation built up at the head of the PV panel system in the presented design.

### Acknowledgement

The authors would like to acknowledge the financial contribution made by the Centre for Engineering and Industrial Design, Waikato Institute of Technology towards the research in this paper.

### References

- [1] Boukhriss, Mokhless, Kamel Zarzoum, Med Ali Maatoug, and Mahdi Timoumi. "Innovation of Solar Desalination System Coupled with Solar Collector: Experimental Study." *Journal of Advanced Research in Fluid Mechanics and Thermal Sciences* 80, no. 1 (2021): 94-111. <https://doi.org/10.37934/arfmts.80.1.94111>
- [2] Emeara, Mohamed S., Ahmed Farouk AbdelGawad, and Ahmed H. El Abagy. "A Novel Renewable Energy Approach for Cairo International Airport "CIA" based on Building Information Modeling "BIM" with Cost Analysis." *Journal of Advanced Research in Fluid Mechanics and Thermal Sciences* 85, no. 2 (2021): 80-106. <https://doi.org/10.37934/arfmts.85.2.80106>
- [3] Nahoui, Azzedine, Redha Rebhi, Giulio Lorenzini, and Younes Menni. "Numerical Study of a Basin Type Solar Still with a Double Glass Cover Under Winter Conditions." *Journal of Advanced Research in Fluid Mechanics and Thermal Sciences* 88, no. 1 (2021): 35-48. <https://doi.org/10.37934/arfmts.88.1.3548>
- [4] Panda, Sudharani, and Rakesh Kumar. "A Review on Heat Transfer Enhancement of Solar Air Heater Using Various Artificial Roughed Geometries." *Journal of Advanced Research in Fluid Mechanics and Thermal Sciences* 89, no. 1 (2022): 92-133. <https://doi.org/10.37934/arfmts.89.1.92133>
- [5] Jubayer, Chowdhury Mohammad, and Horia Hangan. "Numerical simulation of wind effects on a stand-alone ground mounted photovoltaic (PV) system." *Journal of Wind Engineering and Industrial Aerodynamics* 134 (2014): 56-64. <https://doi.org/10.1016/j.jweia.2014.08.008>
- [6] Meroney, Robert N., and David E. Neff. "Wind effects on roof-mounted solar photovoltaic arrays: CFD and wind-tunnel evaluation." In *The Fifth International Symposium on Computational Wind Engineering (CWE 2010)*. 2010.
- [7] Aly, Aly Mousaad, and Girma Bitsuamlak. "Wind-induced pressures on solar panels mounted on residential homes." *Journal of Architectural Engineering* 20, no. 1 (2014): 04013003. [https://doi.org/10.1061/\(ASCE\)AE.1943-5568.0000132](https://doi.org/10.1061/(ASCE)AE.1943-5568.0000132)
- [8] Cao, Jinxin, Akihito Yoshida, Proshit Kumar Saha, and Yukio Tamura. "Wind loading characteristics of solar arrays mounted on flat roofs." *Journal of Wind Engineering and Industrial Aerodynamics* 123 (2013): 214-225. <https://doi.org/10.1016/j.jweia.2013.08.014>
- [9] Bellavia, Carmen. "Light weight molded roof tile with integrated solar capabilities." U.S. Patent 9,038,330, issued May 26, 2015.
- [10] Aly, Aly Mousaad, Chanachock Chokwitthaya, and Raymond Poche. "Retrofitting building roofs with aerodynamic features and solar panels to reduce hurricane damage and enhance eco-friendly energy production." *Sustainable Cities and Society* 35 (2017): 581-593. <https://doi.org/10.1016/j.scs.2017.09.002>
- [11] Alafita, Theresa, and Joshua M. Pearce. "Securitization of residential solar photovoltaic assets: Costs, risks and uncertainty." *Energy Policy* 67 (2014): 488-498. <https://doi.org/10.1016/j.enpol.2013.12.045>

- [12] Branker, Kadra, M. J. M. Pathak, and Joshua M. Pearce. "A review of solar photovoltaic levelized cost of electricity." *Renewable and sustainable energy reviews* 15, no. 9 (2011): 4470-4482. <https://doi.org/10.1016/j.rser.2011.07.104>
- [13] Wittbrodt, B. T., and Joshua M. Pearce. "Total US cost evaluation of low-weight tension-based photovoltaic flat-roof mounted racking." *Solar Energy* 117 (2015): 89-98. <https://doi.org/10.1016/j.solener.2015.04.026>
- [14] Peng, C., Y. Huang, and Z. Wu. "Building-integrated photovoltaics (BIPV) in architectural design in chinaEnergy." *Energy and Buildings* 43, no. 12 (2011): 3592–3598. <https://doi.org/10.1016/j.enbuild.2011.09.032>
- [15] Lu, Hao, and Li-zhi Zhang. "Numerical study of dry deposition of monodisperse and polydisperse dust on building-mounted solar photovoltaic panels with different roof inclinations." *Solar Energy* 176 (2018): 535-544. <https://doi.org/10.1016/j.solener.2018.10.068>
- [16] Whitmore, David William. "Cathodic corrosion protection with solar panel." U.S. Patent 11,105,001, issued August 31, 2021.
- [17] Nakazima, Ichiro, Teruki Hatsukaiwa, Fumihiro Tanigawa, Takuji Nomura, Isao Yoshida, and Kazuhito Hirai. "Roofing tile having photovoltaic module to generate power." U.S. Patent 6,453,629, issued September 24, 2002.
- [18] Nürnberger, Ulf, and Esref Cenk Köse. "Durability of galvanised fasteners in timber construction." *Materials and Corrosion* 71, no. 5 (2020): 834-848. <https://doi.org/10.1002/maco.201911489>
- [19] Fedorova, Anna, Bjørn Petter Jelle, Bożena Dorota Hrynyszyn, and Stig Geving. "Quantification of wind-driven rain intrusion in building-integrated photovoltaic systems." *Solar Energy* 230 (2021): 376-389. <https://doi.org/10.1016/j.solener.2021.10.030>
- [20] Pearce, Joshua M., Jay Meldrum, and Nolan Osborne. "Design of post-consumer modification of standard solar modules to form large-area building-integrated photovoltaic roof slates." *Designs* 1, no. 2 (2017): 9. <https://doi.org/10.3390/designs1020009>
- [21] Baumann, Thomas, Hartmut Nussbaumer, Markus Klenk, Andreas Dreisiebner, Fabian Carigiet, and Franz Baumgartner. "Photovoltaic systems with vertically mounted bifacial PV modules in combination with green roofs." *Solar Energy* 190 (2019): 139-146. <https://doi.org/10.1016/j.solener.2019.08.014>
- [22] Kurnik, Jurij, Marko Jankovec, Kristijan Brecl, and Marko Topic. "Outdoor testing of PV module temperature and performance under different mounting and operational conditions." *Solar Energy Materials and Solar Cells* 95, no. 1 (2011): 373-376. <https://doi.org/10.1016/j.solmat.2010.04.022>
- [23] Nurnberger, Ulf and Kose, Cenk. "Causes and mechanisms of corrosion for supporting structures of rooftop photovoltaic systems." *Otto-Graf-Journal* 18 (2019): 221-238.
- [24] Mani, Monto, B. V. V. Reddy, M. Sreenath, S. Lokabhiraman, and N. Anandrao. "Design of a climate-responsive BIPV research facility in Bangalore." In *Proceedings of ISES World Congress 2007 (Vol. I–Vol. V)*, pp. 356-360. Springer, Berlin, Heidelberg, 2008. [https://doi.org/10.1007/978-3-540-75997-3\\_61](https://doi.org/10.1007/978-3-540-75997-3_61)
- [25] Becerril-Romero, Ignacio, Sergio Giraldo, Simón López-Marino, Marcel Placidi, Yudania Sánchez, Diouldé Sylla, Alejandro Pérez-Rodríguez, Edgardo Saucedo, and Paul Pistor. "Vitreous enamel as sodium source for efficient kesterite solar cells on commercial ceramic tiles." *Solar Energy Materials and Solar Cells* 154 (2016): 11-17. <https://doi.org/10.1016/j.solmat.2016.04.035>
- [26] Siebentritt, Susanne, and Susan Schorr. "Kesterites-a challenging material for solar cells." In *Progress in Photovoltaics: Research and Applications* 20, no. 5, 512–19, 2012. <https://doi.org/10.1002/pip.2156>
- [27] Peters, I. M., and A. M. Nobre. "Deciphering the thermal behavior of floating photovoltaic installations." *Solar Energy Advances* 2 (2022): 100007. <https://doi.org/10.1016/j.seja.2021.100007>
- [28] Grygiel, Piotr, Jan Tarłowski, Marta Przeźniak-Welenc, Marcin Łapiński, Jacek Łubiński, Aleksandra Mielewczyk-Gryń, Krzysztof Mik, Michał Bartmański, Daniel Pelczarski, and Maciej Kwiatek. "Prototype design and development of low-load-roof photovoltaic modules for applications in on-grid systems." *Solar Energy Materials and Solar Cells* 233 (2021): 111384. <https://doi.org/10.1016/j.solmat.2021.111384>